ADVANCED MATERIALS TECHNOLOGIES
www.advmattechnol.de

Characterization, Manipulation, and Isolation of *Paramecium aurelia* Using a Micro-Electromigration Chip and Computer Vision

*Ashaa Preyadharishini Shunmugam and Javier G. Fernandez**

Manipulating microorganisms with inherent motility is a challenging yet significant aim with implications in many biological, environmental, and technological applications. Many microorganisms that are broadly available in nature can be used as self-powered systems that can be directed with external stimuli. *Paramecium* is a unicellular protozoan that exhibits a negative galvanotaxis where the cell follows the direction of weak electric fields. Here, the galvanotactic behavior of *Paramecia* is studied to achieve the precise manipulation of these organisms. Using a specially devised microfluidic chip and computer vision, unprecedented levels of manipulation and isolation of *Paramecia* are demonstrated, enabling their integration, use, and study in micro-electromechanical systems.

Paramecium aurelia is one of the most widespread water organisms, found in large amounts in fresh, brackish, and marine water bodies. *Paramecia* move in water at five times their body length per second,[1] are cultured in simple lettuce and hay infusions, and are ubiquitous organisms in almost any water body around the world. Because of these properties, *Paramecia* are broadly used model organisms in genetics,[2–5] evolution biology,[6–8] and cell biology[9–11] and are a critical biological indicator of water quality.[12–15] Recently, they have also been demonstrated to be a reliable biological model for testing the biocompatibility of new compounds,[16,17] as well as biological models to build propellers.[18]

Despite these broad applications, technologies for the isolation and characterization of *Paramecia* are still based on laboratory techniques from a century ago and are extremely tedious and inefficient. In addition, their lack of development is limiting further uses of *Paramecia*. This deferred technological evolution around *Paramecium*—a common problem in studying many microorganisms—contrasts the enormous development of micrometric tools for mammalian cell studies and isolation that occurred in the last two decades.

Mechanical methods for the isolation of *Paramecia* include picking *Paramecium* from natural water one by one with a pipette,[19] based on the negative geotaxis of swimming organisms,[20] and using antibiotics to establish an axenic culture.[21] The most efficient technique to isolate *Paramecia* is the galvanotaxis of these microorganisms using the methods of van Wagtendonk, Hackett, and Simonsen,[22,23] the main drawbacks of these methods are their large setups and tedious preparation techniques.

Galvanotaxis is an inherent locomotor response to an external electric current shown by various microorganisms. In the case of *Paramecium*, electric fields produce a change in ciliary movement on one of the sides of the organism, inducing an angular momentum on the organism and driving *Paramecia* to move in the direction of the field. While this unique galvanotaxis of *Paramecia* is mostly used for their isolation from other microorganisms,[24] as we demonstrate here, it is also a suitable tool for their integration in micro-electromechanical systems (MEMS).

Here, we present a modernized microfluidic device to characterize and manipulate *Paramecia*, making use of galvanotaxis, microfluidics, and computer vision. Our results demonstrate the integration of the electro-actuation of *Paramecia* in bioMEMS. We demonstrate the capabilities of the proposed system and its potential in future applications in using it to isolate a wild population of *Paramecia* from a local pond, effectively reducing the size of the current method based on a 0.5 m combination of beakers, glass pipes, and saline solutions to a device of less than 2 cm using natural water. Further applications include the production of data for fundamental biological studies, incorporation of mobile microorganisms in MEMS, and environmental measurements.

The device presented herein consists of a microfluidic channel made of silicone-based polymer sealed with a microscope glass slide, enabling its use in any standard optical microscope. At the middle of the microfluidic channel, a 1-mm wide chamber hosts two opposing electrodes, enabling the production and regulation of an electric field perpendicular to the flow of the water sample containing *Paramecia* (Figure S1, Supporting Information). The flow pattern and electric field in the chip, the main components used to manipulate the *Paramecia*, are controlled by a micropump and a power supply, respectively, and are characterized using finite element analysis (FEA). The characterization of the microorganisms was performed using a combination of object recognition and motion tracking using

A. P. Shunmugam, Prof. J. G. Fernandez
Engineering Product Development
Singapore University of Technology and Design
8 Somapah Road, Singapore 487372, Singapore
E-mail: javier.fernandez@sutd.edu.sg

The ORCID identification number(s) for the author(s) of this article can be found under https://doi.org/10.1002/admt.202000152.

DOI: 10.1002/admt.202000152

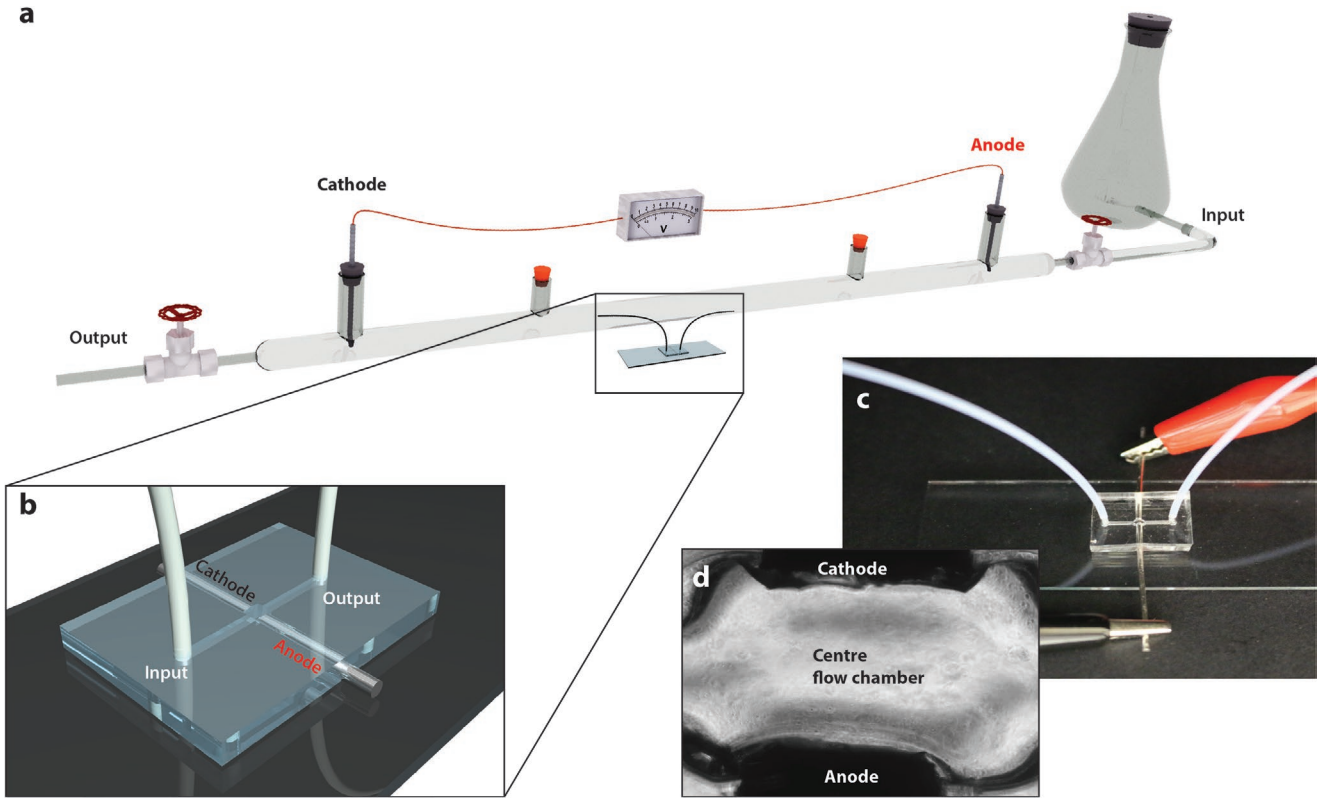

Figure 1. Electromigration chip. a) Electromigration tube commonly used to isolate *Paramecia* by electromigration, first developed by van Wagtendonk in 1949. For a size comparison, the electromigration chip presented herein can be seen beside it. In the proposed system, the 50-cm long tube holding the electrodes was reduced to a 1-mm chamber. b) The electromigration chip; the functional elements were labeled. c) Picture of the actual chip, with the electrical and fluidic connections. d) Image of the central chamber in the electromigration channel as observed with a standard inverted microscope with a 5× lens.

images that were recorded with an inverted light microscope. We believe this device will enable a broader understanding and use of these versatile microorganisms in bioMEMS and other applications by facilitating their manipulation and characterization with unprecedented simplicity and accuracy.

Figure 1a shows a schematic of the electromigration apparatus that is typically used in current research to isolate *Paramecia*[25] compared to the micro-electromigration chip presented herein. Briefly, the current isolation system is comprised of a long glass tube and a conical flask filled with washing fluids. Two electrodes are inserted near the entry and exit of the glass tube. A suspension containing *Paramecia* is introduced through one of the arms, and, upon application of an electric field through the glass tubes, *Paramecia* slowly migrate to the opposing arm following the electric field, where they are removed with a sterile syringe. Figure 1b shows a close-up sketch of the device presented herein. Figure 1c shows the actual fabricated chip, which comprises a polydimethylsiloxane (PDMS) microfluidic chip attached to a standard microscope glass slide. The microfluidic chip has a central flow chamber (Figure 1d) with electrodes placed vertically on both sides. When the sample passes through the central flow chamber, an electric field is applied to the fluid inside the chamber, enabling the control of the *Paramecia* by slowing, stopping, or diverting its movement based on field intensity and timing. Therefore, the movement of *Paramecia* in the central chamber is determined by the combined effect of the electric field across the electrodes and the perpendicular laminar flow. Making use of a microfluidic system enables data acquisition and analysis at single-cell level. Compared to traditional separation techniques, this feature is in detriment of the volume of sample processed at a given time, due to the smaller processing chamber. Despite this, the proposed system enabled the processing (and analysis) of larger samples than traditional techniques, due to the fact that it enabled the automatization for processing arbitrarily large volumes of a sample. In the proposed system, the isolated *Paramecium* can be trapped in the central chamber, the sample input switch to clean water/sample, the field released, and the paramecium collected at the output before the input switched back to the sample to repeat the process. This example of collection method, manually produced here, is easily automatable with a 3-way valve, enabling the process of virtually unlimited volumes without disassembling the experimental setup or human intervention. In contrast, traditional techniques require the emptying and reloading of the separation chamber/tube after each sample.

Results of the stationary FEA study for the stabilized flow and field are presented in **Figure 2**, while boundary conditions are presented in Figure S2, Supporting Information. The analysis of the hydraulic flow in the microchannel produced the expected laminar flow behavior, as shown in Figure 2a,b. The fluid flow in the test chamber was divided into two regions:

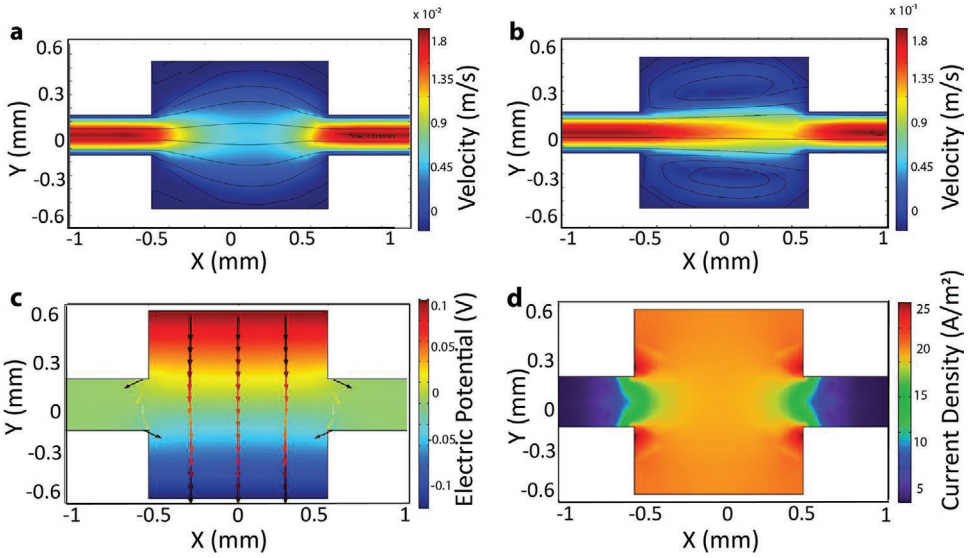

Figure 2. Finite Element Analysis of the *XY*-plane of the central chamber of the microfluidic channel. a) Simulation of the flow analysis at 10 µL min^{-1}, showing how the flow velocity is reduced at the center of the chamber. b) Simulation of the flow analysis at 100 µL min^{-1}, showing a similar flow pattern, where the central area of the laminar flow is sandwiched between the two stagnant sides. c) Characterization of the applied field potential and the electric field generated inside the chip. d) Analysis of the modulus of the electric field inside the chamber.

the central region equal to the width of the input channel and the side regions on top and bottom of the chamber. When studying variations of different flow patterns, some significant differences can be observed in the central area of the chamber. Negligible changes were seen in the top and bottom regions, except for a weak vortex observed to form at flow rates beyond the feasibility of the system, remaining these regions stagnant beyond the low and high flow rates used here (Figure S3, Supporting Information). This particularity allowed for the isolation of *Paramecia* from a mixed sample. Under the influence of an electric field, *Paramecium* tends to abandon the strong laminar flow toward stagnant areas, while the rest of the particles and microorganisms showed similar galvanotaxis and exited the chamber without leaving the central stream. At the side regions, *Paramecium* can be manipulated further by applying the electric field without the influence of the fluid flow. The dimensions of stagnant areas are chosen such they are large enough to accommodate the isolated *Paramecium*, but also small enough to avoid the use very large voltages to establish the electric field, which result in higher temperatures and water hydrolysis.

Galvanotaxis in *Paramecium* is a response occurring only in a limited range of electric fields; in low fields, *Paramecium* does not have an apparent response to the field, while, in high fields, secondary effects, such as the blocking of ion channels, resulting in random responses and, ultimately, the death of microorganisms. The simulation of the electrical and dynamic characteristics of the central chamber enabled matching the electrical characteristics of the region to previously reported electric fields that are susceptible to the induction of galvanotaxis in *Paramecium*. For the 1-mm wide chamber in this study, the platinum electrodes were provided with a potential difference ranging from 2.2 to 2.6 V. The analysis of the field pattern at these voltages revealed the expected homogenous field between the electrodes similar to a parallel plate capacitor and perpendicular to the flow (Figure 2c) with only some variation in terms of the proximity of the inlet and the outlet (Figure 2d).

For the analysis of the galvanotaxis of *Paramecia* in the microfluidic chip, about 1000 *Paramecia* were recorded, with an average of 200 data points per *Paramecium* tracked during the time the *Paramecia* spent in the central chamber of the device. To our knowledge, this amount of data makes this experiment the largest study on the electromigration of a microorganism ever produced. **Figure 3**a displays the object recognition algorithm built in MATLAB, which was used to identify and label the *Paramecia* upon entering the chamber (yellow box). The movement of the *Paramecia* was tracked at 30 frames per s. The movement of each *Paramecium* in each frame was recorded, and the subsequent position was estimated. The estimated position was used to identify individual *Paramecium* from frame to frame, even when a *Paramecium* was missed during several frames due to video artifacts or due to overlap with other *Paramecia* (Video S1, Supporting Information). Figure 3b shows three paths of three *Paramecia* under the influence of different flow rates and voltages. At a flow rate of 16 µL min^{-1} and an intermediate voltage of 2.5 V, the *Paramecia* did not deviate from the central flow and transferred early from the chamber (purple path). In the absence of an electric field, flow rates below 6 µL min^{-1} resulted in high degrees of freedom for the *Paramecia* (green path). At the optimal flow rate of 8 µL min^{-1} and a voltage of 2.5 V, the *Paramecia* stayed near the electrodes (red path, Figure 3d). Figure 3c shows the typical data acquired after 10 min of video. Each color represents the path of one *Paramecium*.

The object tracking system is explicitly tailored for *Paramecium* and therefore ignores all entities not recognized as one. The ability of the electromigration chip to retain *Paramecia* under the influence of an external electric field was measured by comparing the time spent by the *Paramecia* inside the central chamber at different field intensities and flow rates (shown

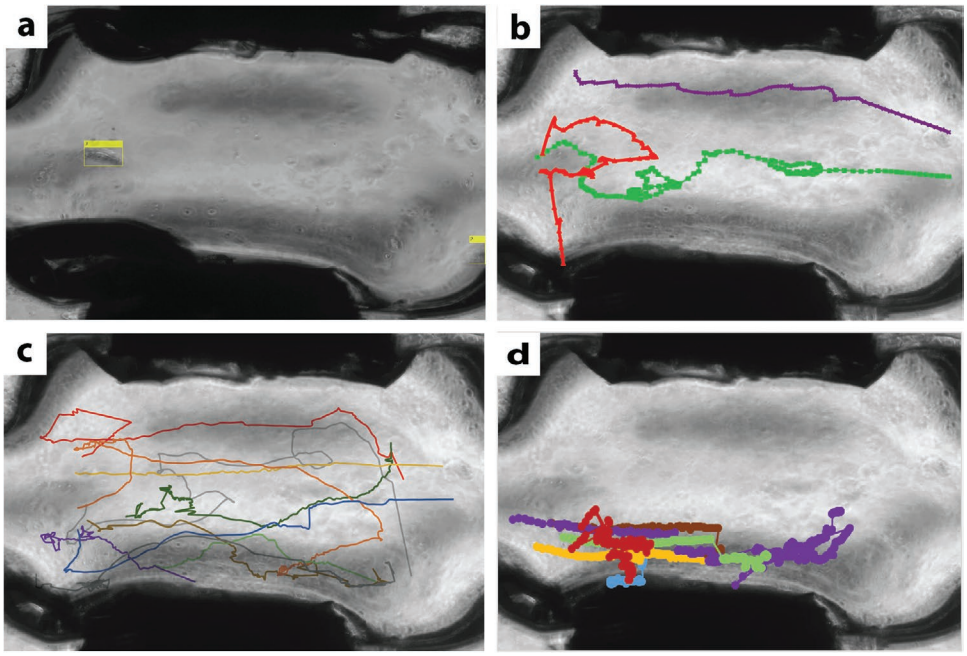

Figure 3. *Paramecia* tracking and data acquisition. a) Image of the object recognition and tracking of the *Paramecia*. The *Paramecia* were detected upon entering the chamber and boxed for easy identification. Unique identifications were displayed in the box to easily find the *Paramecia* as well as manually remove false positives. b) Image shows the paths of three different *Paramecia* tracked under different experimental conditions. Each color corresponds to a path followed by a *Paramecium*. The purple path represents the path of a *Paramecium* at a flow rate of 12 μL min^{-1}, the green path represents the path of a *Paramecium* at a medium flow rate without voltage applied (8 μL min^{-1}), and the red path represents the path of a *Paramecium* at an optimal flow rate and voltage (8 μL min^{-1} and 2.5 V). c) Image shows the typical data acquired after 10 min of video. d) Image shows the paths followed by six *Paramecia* escaping the flow and settling down inside the central chamber. Each color corresponds to the path of one *Paramecium*.

in **Figure 4**a). Flow rate of 12 μL min^{-1} showed a decline in the total time spent by the microorganism in the chamber since it traversed through the central chamber rapidly ignoring the electric field. Flow rate of 8 μL min^{-1} provided the optimal flowrate, giving the maximum time spent inside the chamber. Besides that, rise in the applied voltage, resulted in increase in the time spent in the chamber with a maximum time spent seen at a voltage of 2.5 V with further increase in the voltage resulted in the death of the *Paramecia*, which contributed to a decrease in the total time spent by *Paramecia* in the central chamber.

The second parametrization of the movement of the *Paramecia* was based on the horizontal speed of the *Paramecia* in the chip. The calculated average speed was plotted versus the voltage applied across the electrodes at each flow rate, as shown in Figure 4b. In agreement with the observation in the previous section, the applied voltage was inversely proportional to the speed of the movement of the *Paramecia* on the *X*-axis. At 12 μL min^{-1} flow rates, the horizontal movement was largely conditioned by the flow, while the effect of the field was negligible; however, for all flow rates below 12 μL min^{-1}, the horizontal movement was clearly hindered at a voltage of 2.4 to 2.5 V, where, in agreement with previous observations, the susceptibility of *Paramecia* to galvanotaxis seemed to be maximized.[26] In the absence of electric field (i.e., 0 V in Figure 4b), as the flow rates decreases from 12 to 6 μL min^{-1}, the ability of the *Paramecia* to move freely also resulted in an observed decrease in the overall horizontal speed.

The paths of the *Paramecia* and their positions inside the chamber were also considered. The chamber was divided into the two regions arising from the fluidic studies: one central area of a similar width as the input and output channels (i.e., area under the influence of the laminar flow), and a second area combining the two stagnant areas at the sides of the chamber (i.e., area outside the laminar flow). The occurrence of *Paramecia* at these regions was plotted for the different flow rates and voltages, as shown in Figure 4c. At lower flow rates like 8 μL min^{-1}, the occurrence of *Paramecia* at the side regions increased with the applied voltage, reaching its maximum at 2.5 V and decreasing at 2.6 V when the side effects of the intense electric field hindered the effect of galvanotaxis. At flow rates higher than 8 μL min^{-1}, the occurrence of Paramaecia in the side areas of the chip greatly decreased due to the inability of the *Paramecia* to escape the laminar flow. Similar to the previous two analyses, optimal separation conditions occurred at a flow rate of 8 μL min^{-1} and a voltage of 2.5 V, when the majority of the *Paramecia* were removed from the central stream. This optimal current, corresponding to a field of 2.27×10^3 V m^{-1}, is in agreement with the range of fields reported to maximize galvanotaxis of *Paramecia* in traditional devices.[26] In static conditions (i.e., without flow or electric field), *Paramecia* are free to move in the central chamber. Since the region categorized as "side areas" (i.e., stagnant) is twice the central area, in static conditions the occurrence of *Paramecia* in the side areas is twice more substantial than in the central region. Despite this, even at low flow of 6 or 8 μL min^{-1}, *Paramecia* seem to be strongly conditioned by the flowrate, spending 80% of its time

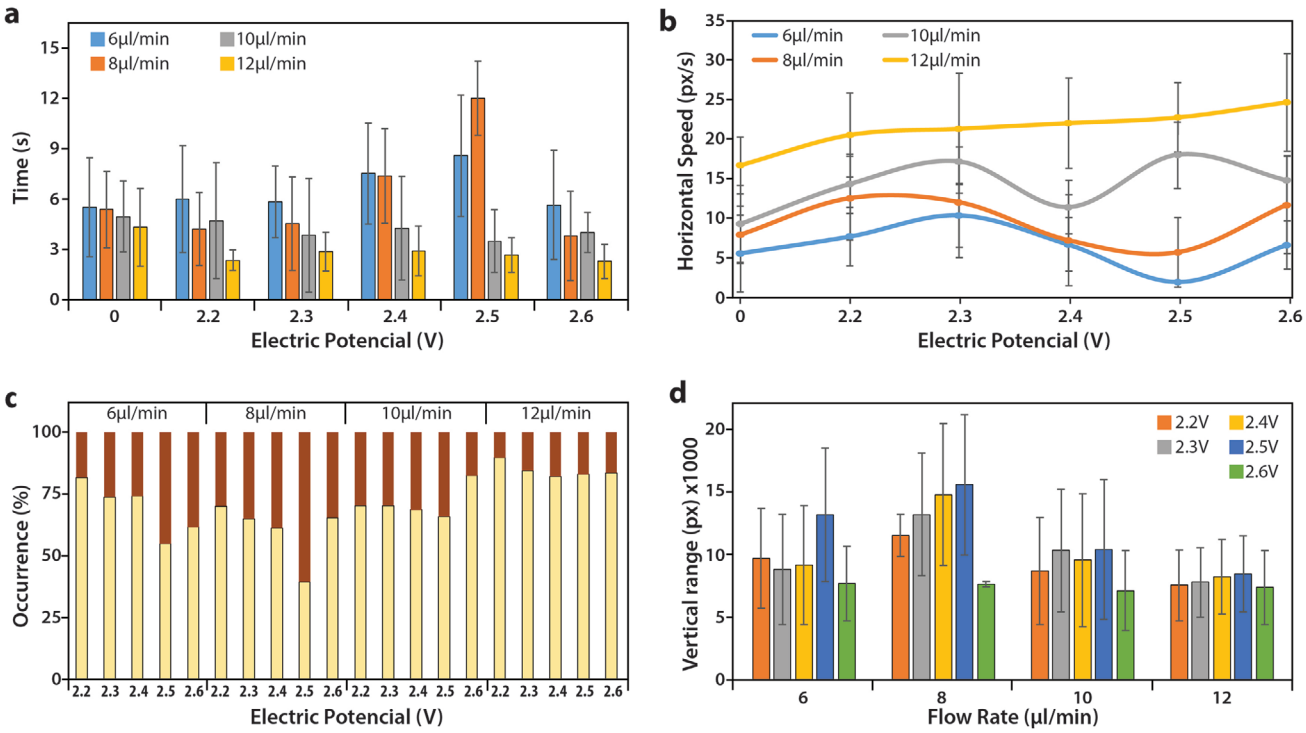

Figure 4. Quantitative analysis of the isolation chamber. a) Plot of the time spent by the *Paramecia* in the chamber versus the flow rates grouped at the different applied voltages. It shows a gradual decrease in the pattern, indicating that, as the flow rate increases, the time spent decreases. The flow rate of 8 µL min^{-1} gives the maximum time spent in the chamber. In addition, a gradual increase is seen in the pattern of applied voltages, indicating that, as voltage increases, the time spent also increases. An applied voltage of 2.5 V gives the maximum time taken by the *Paramecia*. b) Graph plotted for speed on the *X*-axis versus the voltage applied at different flow rates. The horizontal speed appears directly correlated to the flow; a minimum of speed is found for all the flows at about 2.4–2.5 V when galvanotaxis is at a maximum and the *Paramecia* move vertically toward the electrodes. At a flow rate of 12 µL min^{-1}, almost no difference is observed, confirming the inability of the *Paramecia* to oppose such a maximum. c) Histogram of the frequency of the position of the *Y*-axis as a percentage versus the applied voltages grouped by flow rate. Red represents the side regions of the chamber, while yellow represents the central area of the thickness similar to the inlet and the outlet. The ability of the chip to separate the *Paramecia* from the central flow by galvanotaxis is at its maximum at 8 µL min^{-1} and a voltage of 2.5 V. d) Graph plotted for the variance of the *Y*-axis versus the voltage at each flow rate. At a flow rate of 12 µL min^{-1}, the voltage has no significant difference in terms of the vertical variance, whereas, at flow rates of 8 µL min^{-1}, variance increases with an increase in the voltage. All error bar denotes the standard deviation.

in the narrow space under the influence of the laminar flow (i.e., central area, Figure 4c).

The last component analyzed was the mobility of the *Paramecia* in the *Y*-axis. This magnitude correlates with the ability of the system to constrict the movement of the *Paramecia* by either the flow or the field. The calculated average of the variance is represented in Figure 4d. As expected at flow rates of 12 µL min^{-1}, the *Paramecia* were unable to abandon the central flow of the chamber, resulting in an almost fixed vertical position and, therefore, a low variance even in high-intensity fields. Interestingly, as observed before, the ability of the *Paramecia* to swim starts decreasing at voltages higher than 2.5 V, resulting in a low vertical variance even at low flow rates of 8 µL min^{-1} when the *Paramecia* should have been able to move almost freely in the chamber. Therefore, as observed in the previous data, in the conditions tested the flow rate of 8 µL min^{-1} and the voltage of 2.5 V unequivocally resulted in the highest deflection of the *Paramecia* toward the sides of the chip from the input stream.

Analysis of variance (ANOVA) was performed to check the statistical significance of the obtained results. The effects of the flow rate and voltage were studied using a two-way ANOVA comprising the *Y*-axis variances of all the flow rates as factors/samples with six levels with no voltage and at 2.2, 2.3, 2.4, 2.5, and 2.6 V. From the analysis, the flow rates (p-value = 0.019) and applied voltages (p-value = 4.4×10^{-9}) were confirmed to strongly determine the movement of the *Paramecia* in the microfluidic chip.

The device presented herein represents a powerful tool that can obtain large amounts of data to study *Paramecia*. It can also be used to control these highly mobile organisms for their isolation from natural samples of water.

In this case, the *Paramecia* were segregated from other particles and microorganisms in a water sample from a local pond by forcing the former to escape the central laminar flow in the chamber. For the isolation of *paramecia,* we injected the sample at 8 µL min^{-1} during five minutes in the chip, swapped the sample input by clean water, and switched off the (2.5 V) current, and collected the (now clean) retained paramecia at the output (**Figure 5**). We repeated this process five consecutive times. Every five minutes, one to eight *paramecia* entered the chamber with an average 81.42 ± 18.45% of them retained there and recovered at the output. However, this efficiency dropped to 72.72% when the 25 min (i.e., five cycles) were

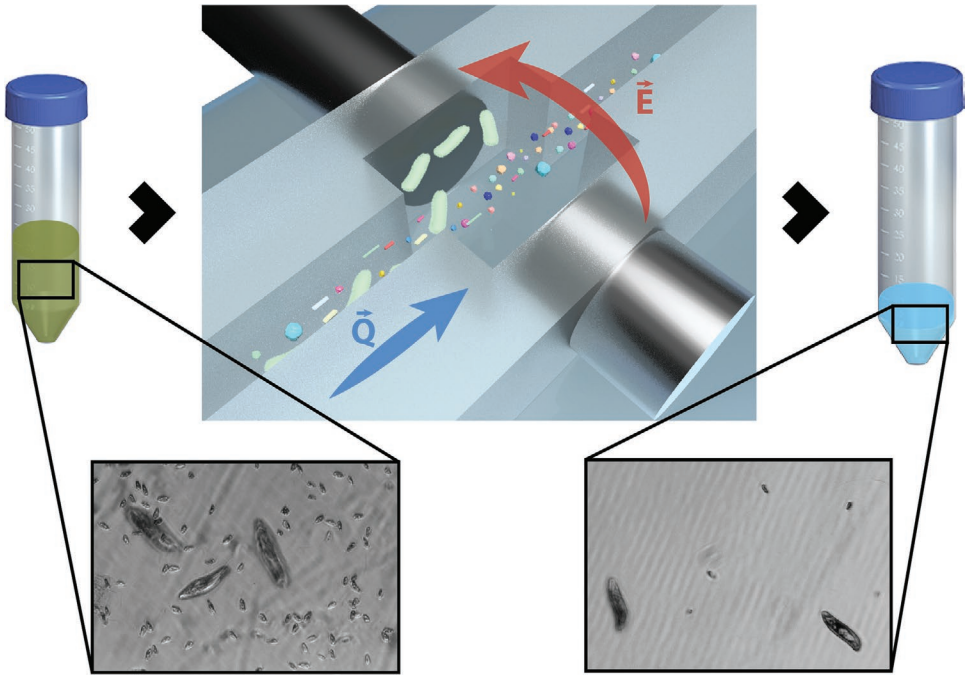

Figure 5. Trapping efficiency of the electromigration chamber. A sample of natural water from a local pond was loaded in the chip. The water sample containing *Paramecium* and many other microorganisms and particles was loaded using a syringe pump (image shown on the left side was taken before loading into the microfluidic chip). Upon reaching the central chamber, the laminar flow forced the sample to traverse and exit from the output with a minimum disturbance of the flow. In the presence of external voltage, the *Paramecia* were segregated into the chamber. The *Paramecia* were retained in the chamber, while the inlet was changed from the original sample to clean water. When the voltage was released, the isolated *Paramecia* were recovered at the output (image shown in the right side was taken after collecting the isolated *Paramecium* from the system). The efficiency of the electromigration chamber (i.e., ratio of the total amount of *Paramecia* entering the chamber and *Paramecia* recovered from the system) was of 72.72%. In the diagram, the *paramecia* and other particles are drawn out of scale for representation purposes.

considered as a single experiment. The efficiency in separating and collecting *Paramecia* from natural water samples, measured as the ratio between the *Paramecia* gathered at the output after switching to clean water, and the total amount of *Paramecia* introduced, was measured using the computer vision setup described above. The collected *Paramecia* were transferred to an infusion media where they rapidly multiplied, demonstrating the viability of the organisms.

In summary, an electromigration channel was successfully designed and fabricated. Several analyses were performed to characterize the channel and display the movement of *Paramecia* inside the microchannel in the presence of an electric field. An FEA of the flow rate and electric field was conducted to determine the physiological conditions of the proposed electromigration chip. The retention time of the *Paramecia* inside the central chamber of the device, the progression of the movement of *Paramecia* on the *X*-axis, the recurrence of the position of *Paramecia* on the *Y*-axis, and the deviation of the position of *Paramecia* on the *Y*-axis were studied and plotted using computer vision as a method to register large amounts of data on *Paramecium* behavior autonomously. An extensive analysis was conducted to determine the ideal conditions to isolate a wild population of *Paramecia* from other microorganisms and particles, demonstrating a 73% success rate to retain and isolate all *Paramecia* entering the electromigration chip. The above-presented method includes a combination of characteristics of simultaneous single-cell analysis with high throughput. We believe this work is an important step toward the development of micrometric tools specifically tailored for highly mobile microorganisms, enabling not only more accurate and data-intensive studies, but also the integration of these versatile cells into bioMEMS,[27,28] including biological robots[29] and environmental sensors.[30]

Experimental Section

Materials: The *P. aurelia* was purchased from Nantah Capital One Pvt. Ltd. (Singapore). Lettuce infusion prepared by boiling lettuce leaves in water was used to maintain the *Paramecium* culture. *Paramecia* grown along with other microorganisms were taken together for the experiments. The PDMS was purchased in a SYLGARD 184 Silicone Elastomer Kit (Dow Chemical Company, USA) from Tatlee Engineering Pte Ltd. (Singapore). The platinum electrodes were bought from Surepure Chemetals Inc. (USA).

3D Modeling and Printing the Mold: The 3D diagram of the mold of the microfluidic chip was designed using SOLIDWORKS (Dassault Systèmes, France). A J750 3D Printer (Stratasys, USA) was used to print the desired mold design. A combination of materials VeroClear and TangoPlus (Stratasys, USA) was used to print the samples. A layer of support material (SR-20, Stratasys, USA) was used between the surface of the stage and the actual mold. Once the mold was printed, the extra support layer was peeled off the mold.

The 3D printed mold was scraped off the support material and soaked in water overnight to remove any extra support material present on the surface. Then, the mold was dried in an oven at 60 °C for 2–3 h.

Microchannel Production: PDMS, a silicon-based organic polymer, was used for the fabrication of the microfluidic chips. From the SYLGARD 184 Silicone Elastomer Kit, 10 parts of the base were combined with 1 part of the curing agent and mixed thoroughly. The air bubbles that formed during the mixing process were discarded by placing the mixture in the desiccator. The mixture was then poured into a small Petri dish with the dried mold and left in an oven at 60 °C for 24 h to cure. The rectangular part of the microchannel was cut from the rest of the casting.

Electromigration Chip Fabrication: The platinum electrodes were inserted vertically into the microchannel, so that when sample liquid was passed through the central chamber, the edges of the electrodes were in contact with the liquid. Platinum was chosen because of its resistance to corrosion and hydrolysis. The fabricated chip with the electrodes and a clean glass slide were plasma-treated to bond them together irreversibly forming the microfluidic chip. To make the bonds stronger and leak proof, it was then kept at 100 °C for 15 min. Then, tubings were inserted at the ends of the channels for the sample to flow in and out. Water was passed through the channel to make sure that the fabricated chip was leak-free.

Simulation of the Microchannel: COMSOL Multiphysics (COMSOL Inc., Sweden) was used to simulate the effect of fluid flow inside the chamber. The fabricated chip was examined using FEA to parametrize the electrical and fluid conditions in the chamber. It is important to note that, due to the low concentration of microorganisms in the water sample, the sample was deliberately not treated as an active fluid and the influence of the turbulent effects generated by the self-propelled *Paramecia* on their (nonexistent) neighbors was neglected. Simulation of fluid flow was done to narrow down the flowrate range for the actual hands-on experiments to be carried out. The electric field was also simulated using COMSOL Multiphysics.

Simulation of applied voltage was done to check whether the design of the galvanotactic chip could convert the voltage into electric field across the chamber between the electrodes. The chosen values of voltage ranged from 2.2 to 2.6 V with a net current of approximately 0.1–0.25 mA, based on the previous literature values from the electromigration of *Paramecia*, where the net current used was similar.[26]

Microchannel Use and Data Collection: When *Paramecium* was made to flow through the microfluidic chip's central chamber, in the presence of electric field, the microorganisms got deflected away from the sample flow and got pulled to the sides of the chamber near the cathode. This trend was used to segregate *Paramecia* by concentrating them on the sides of a microfluidic chamber in the presence of the electric field, and then collected by turning off the electric field and switching the sample with clean media. Sample liquid containing the *Paramecia* was passed through the microfluidic channel at different flow rates and electric voltages. The experiments were recorded using an inverted light microscope (Axio Observer, Carl Zeiss, Germany) and a custom-built camera. The videos were recorded at 15 frames per s. The analysis was conducted using a customized script in MATLAB (MathWorks, USA), making use of its Vision and Image Analysis toolboxes. The videos were processed at each frame using a Kalman filter to locate the object (i.e., *Paramecium*) and a path predictor to generate the data. Each object identified was assigned a unique ID and tracked in consecutive frames. Paths with short lives were discarded as noise. Using a path prediction algorithm enabled the more accurate identification of individual *Paramecium* and allowed the recapture of a *Paramecium* path after it was lost for several frames (e.g., when a *Paramecium* moved too close to the edge of the chamber). All the data were stored as separate files containing the (x, y) coordinates in each frame.

Data Analysis: From the data collected, several parameters were studied to quantify and compare the movement of *Paramecia* under different experimental conditions. a) The first parameter studied was the retention time to understand how long *Paramecia* stayed in the chamber. The duration that 30 different *Paramecia* stayed in the chamber was studied. The different factors considered for this analysis were the flow rates, ranging from 6 to 12 µL min^{-1}, and the applied voltage, varying from 2.2–2.6 V. b) The second parameter studied was the progression in the *X*-direction in order to measure the influence of the flow on the free movement of the *Paramecia*. When a *Paramecium* moved toward electrodes and settled at their sides, its movement was in the perpendicular direction, and horizontal displacement was reduced. This was calculated by collecting *X*-component values from the movement of the first 30 *Paramecia* entering the chamber. The speed was calculated for each *Paramecium*, and the average speed of all 30 *Paramecia* was used for the analysis. c) The third parameter studied was the relative vertical position of the *Paramecia* in the chip to assess the movement of *Paramecia* inside and outside the laminar flow. In the presence of an electric field, the *Paramecia* were deflected to the sides of the chamber. By parametrizing the chamber as an *XY*-plane using the pixel coordinates, the movement of the *Paramecia* in the presence of electric field could be classified as the time they spent outside the flow. d) The fourth parameter studied was the variability of the vertical position of the *Paramecia*. This variability of the *Y*-axis was related to both the ability of the electric field to extract *Paramecia* from the central flow and the ability to retain *Paramecia* in the proximity of the electrode once extracted. As a result, flow rates of 6 µL min^{-1} had little influence on the movement of *Paramecia*, resulting in random movements, thereby creating a large variance on their vertical position. However, with an increase in the flow rate, the movement of the *Paramecia* was contained within the middle region of the chamber. Therefore, there was a decreased variance of the vertical position of *Paramecia* in the central chamber.

In addition, the applied voltage had an effect on the movement that made the *Paramecia* settle toward the electrodes. This resulted in a higher variance on the *Y*-axis. Therefore, variance on the *Y*-axis enabled the study of the combined effect of the flow rate and the electric field. The *Y*-component was collected randomly from 30 *Paramecia*, and its variance was calculated. The average variance was calculated for each condition and plotted into a graph.

Trapping Efficiency: A sample of water from a local pond was used as a real model to test the efficiency of the system. The sample was introduced in the system using a syringe. The efficiency of the isolation was calculated as the ratio of total number of *Paramecia* traversing the system (measured using an inverted microscope) and the number of those being recovered at the output of the system after switching the sample liquid to media. Efficiency calculation was repeated five times and the average efficiency of the electromigration chamber was reported as the average of them.

Supporting Information

Supporting Information is available from the Wiley Online Library or from the author.

Acknowledgements

This work was partially supported by the SUTD-MIT International Design Center and the Ministry of Education, Singapore (Grant number: MOE2018-T2-2-176).

Conflict of Interest

The authors declare no conflict of interest.

Keywords

computer vision, electromigration, galvanotaxis, micromanipulation, *Paramecia*

Received: February 24, 2020
Revised: May 2, 2020
Published online: June 3, 2020

[1] R. S. Fearing, in *Proc. of 2nd Int. Symp. Micromachines and Human Sciences*, Nagoya, Japan **1991**.
[2] M. He, J. Wang, X. Fan, X. Liu, W. Shi, N. Huang, F. Zhao, M. Miao, *ISME J.* **2019**, *13*, 1360.
[3] X. Lu, E. Gentekaki, Y. Xu, L. Huang, Y. Li, X. Lu, Y. Zhao, X. Lin, Z. Yi, *Eur. J. Protistol.* **2019**, *67*, 142.
[4] L. Madeddu, C. Klotz, J. P. le Caer, J. Beisson, *Eur. J. Biochem.* **1996**, *238*, 121.
[5] J.-M. Aury, O. Jaillon, L. Duret, B. Noel, C. Jubin, B. M. Porcel, B. Ségurens, V. Daubin, V. Anthouard, N. Aiach, O. Arnaiz, A. Billaut, J. Beisson, I. Blanc, K. Bouhouche, F. Câmara, S. Duharcourt, R. Guigo, D. Gogendeau, M. Katinka, A.-M. Keller, R. Kissmehl, C. Klotz, F. Koll, A. le Mouël, G. Lepère, S. Malinsky, M. Nowacki, J. K. Nowak, H. Plattner, et al., *Nature* **2006**, *444*, 171.
[6] J.-F. Gout, P. Johri, O. Arnaiz, T. G. Doak, S. Bhullar, A. Couloux, F. Guérin, S. Malinsky, L. Sperling, K. Labadie, E. Meyer, S. Duharcourt, M. Lynch, *bioRxiv* **2019**, 573576, https://doi.org/10.1101/573576.
[7] A. B. Duncan, S. Fellous, O. Kaltz, *Evolution* **2011**, *65*, 3462.
[8] P. H. Harvey, M. D. Pagel, *The Comparative Method in Evolutionary Biology*, Oxford university press, Oxford **1991**.
[9] J. Godau, L. P. Ferretti, A. Trenner, E. Dubois, C. von Aesch, A. Marmignon, L. Simon, A. Kapusta, R. Guerois, M. Betermier, A. A. Sartori, *DNA Repair* **2019**, *77*, 96.
[10] M. Lefort-Tran, K. Aufderheide, M. Pouphile, M. Rossignol, J. Beisson, *J. Cell Biol.* **1981**, *88*, 301.
[11] J. T. Francis, T. M. Hennessey, *J. Eukaryot. Microbiol.* **1995**, *42*, 78.
[12] M. Castelli, E. Sabaneyeva, O. Lanzoni, N. Lebedeva, A. M. Floriano, S. Gaiarsa, K. Benken, L. Modeo, C. Bandi, A. Potekhin, D. Sassera, G. Petroni, *ISME J.* **2019**, *13*, 2280.
[13] L. Jiang, P. J. Morin, *J. Anim. Ecol.* **2007**, *76*, 660.
[14] M. Hori, M. Fujishima, *J. Eukaryot. Microbiol.* **2003**, *50*, 293.
[15] L. Jiang, J. A. Krumins, *Ecol. Res.* **2006**, *21*, 723.
[16] F. Basavand, M. Karami, R. Mohammadi, *Adv. Sci. Eng. Med.* **2019**, *11*, 178.
[17] N. Miyoshi, T. Kawano, M. Tanaka, T. Kadono, T. Kosaka, M. Kunimoto, T. Takahashi, H. Hosoya, *J. Health Sci.* **2003**, *49*, 429.
[18] A. Nematollahisarvestani, A. Shamloo, *Prog. Biophys. Mol. Biol.* **2019**, *142*, 32.
[19] T. M. Sonneborn, *J. Exp. Zool.* **1950**, *113*, 87.
[20] W. J. van Wagtendonk, A. T. Soldo, in *Methods in Cell Biology* (Ed: D. M. Prescott), Academic Press, Cambridge **1970**, p. 117.
[21] S. L. Allen, T. A. Nerad, *J. Protozool.* **1978**, *25*, 134.
[22] W. J. van Wagtendonk, P. L. Hackett, *Proc. Natl. Acad. Sci. USA* **1949**, *35*, 155.
[23] W. J. V. Wagtendonk, D. H. Simonsen, L. P. Zill, *Physiol. Zool.* **1952**, *25*, 312.
[24] S. Wagener, C. K. Stumm, G. D. Vogels, *FEMS Microbiol. Lett.* **1986**, *38*, 197.
[25] W. van Wagtendonk, P. L. Hackett, *Proc. Natl. Acad. Sci. USA* **1949**, *35*, 155.
[26] A. Itoh, *IEEE/ASME Trans. Mechatron.* **2000**, *5*, 181.
[27] I. H. Riedel-Kruse, A. M. Chung, B. Dura, A. L. Hamilton, B. C. Lee, *Lab Chip* **2011**, *11*, 14.
[28] K. Otsuka, S. Maruta, A. Noriyasu, K. Nakazawa, T. Kawano, *Advanced Materials Research*, Trans Tech Publications, Switzerland **2014**.
[29] R. Mayne, J. G. H. Whiting, G. Wheway, C. Melhuish, A. Adamatzky, *Biosystems* **2017**, *156*, 46.
[30] T. Kawano, *Advanced Materials Research*, Trans Tech Publications, Switzerland **2014**.